Extrapolated Projection Methods for PAPR Reduction

Jochen Fink, Renato L.G. Cavalcante, Peter Jung, Slawomir Stanczak

Wireless Communications and Networks
Fraunhofer Heinrich Hertz Institute Berlin, Germany
{jochen.fink, renato.cavalcante, peter.jung, slawomir.stanczak}@hhi.fraunhofer.de

Abstract—Over more than the last decade, there has been a significant effort in research to reduce the peak-to-average power ratio (PAPR) in orthogonal frequency-division multiplexing (OFDM) systems. This effort has been mainly driven by the need for enhancing the efficiency of power amplifiers. In this paper, we formulate the PAPR reduction problem as a feasibility problem in a real Hilbert space, and provide algorithmic solutions based on extrapolated projection methods with suitably constructed constraint sets. This set-theoretic approach provides a high flexibility and includes various existing PAPR reduction techniques as special cases. In particular, it allows for balancing between the spectral efficiency and signal distortion on a symbol-to-symbol basis, while supporting arbitrary combinations of quadrature amplitude modulation (QAM) constellations. Moreover, we extend the proposed approach to reuse the phase of pilot subcarriers that are simultaneously used for channel estimation. Simulations show remarkable performance gains resulting from extrapolation, which makes it possible to achieve a considerable PAPR reduction in just a few iterations with low computational cost.

Index Terms—Extrapolated projection methods, OFDM, set-theoretic PAPR reduction

I. INTRODUCTION

Compared with other modulation methods, orthogonal frequency-division multiplexing (OFDM) exhibits a high peak-to-average power ratio (PAPR) [1], [2], which might cause the transmit signal to exceed the linear region of operation of power amplifiers, and thereby introduce undesired signal distortions. Power amplifiers with a large linear region are highly inefficient in terms of both energy consumption and costs, so there has been an enormous research effort directed towards the development of practical PAPR reduction techniques, which include various basic approaches such as coding, interleaving, or selective mapping [3].

In this study, we focus on set-theoretic approaches to the PAPR reduction problem because they open up the door to the development of flexible, low-complexity PAPR reduction techniques that can be easily implemented in state-of-the-art OFDM systems with large numbers of subcarriers and very strict latency requirements. The basic idea behind common approaches to the PAPR reduction problem is to modify the waveform of the transmission signal while satisfying certain constraints such as spectral mask and vector magnitude (EVM) constraints. In general, these constraints depend on parameters that change from symbol to symbol (e.g. allocation of pilot and data subcarriers or constellation size might change between subsequent OFDM symbols), so there is a strong need for PAPR reduction techniques that have enough flexibility to systematically incorporate fast-changing constraints. Against this background, set-theoretic approaches provide a natural framework for dealing with the PAPR reduction problem in modern OFDM systems.

The contribution of this paper can be summarized as follows. We develop a set-theoretic framework for implementing PAPR reduction algorithms that can flexibly combine different frequency-domain constraints and adapt them on a time scale of two consecutive OFDM symbols. In particular, we propose a PAPR reduction algorithm for tone reservation (TR) [4], [5] and iterative clipping and filtering (ICF) [6] (affine/linear frequency constraints) based on the extrapolated alternating projection method (EAPM). In addition, we propose a generalization of this algorithm to non-affine frequency-domain constraints based on the Gurin-Polyak-Raik (GPR) approach [7, Sect. 5.2]. The proposed generalization can deal with arbitrary combinations of constraints related to EVM, spectral masks, active constellation extension (ACE) [2], and compensation subcarriers. Moreover, we present a heuristic extension to incorporate non-convex magnitude equality constraints on compensation subcarriers.

II. PRELIMINARIES

A. Notation

In the following, lower case letters denote scalars, lower case bold letters denote column vectors, and upper case bold letters denote matrices. Complex valued vectors $\underline{\mathbf{a}}$ and matrices $\underline{\mathbf{A}}$ are highlighted by an underscore. The all-zero vector is denoted by $\mathbf{0}$, $\mathbf{e}_i$ denotes the ith unit vector (the vector dimension will be clear from the context), a_k denotes the kth element of vector $\mathbf{a}$, and $\mathbf{I}$ is used to denote an identity matrix. The cardinality of a set $\mathcal{I} \subset \mathbb{N}$ is denoted by $|\mathcal{I}|$, and the expected value of a random variable x is denoted by $E(x)$.

Given a closed set C in a finite dimensional real Hilbert space $\mathcal{H}$ with the norm $\|\mathbf{a}\| := \sqrt{\langle \mathbf{a}, \mathbf{a} \rangle}$ induced by the inner product $(\forall \mathbf{a}, \mathbf{b} \in \mathcal{H})$ $\langle \mathbf{a}, \mathbf{b} \rangle := \mathbf{a}^T \mathbf{b}$, a projection of $\mathbf{x} \in \mathcal{H}$ onto C is a solution to the following optimization problem:

$$\underset{\mathbf{y} \in C}{\text{minimize}} \ \|\mathbf{x} - \mathbf{y}\|. \tag{1}$$

If C is in addition convex, then (1) has a unique solution that we denote by $P_C(\mathbf{x}) \in C$. If C is non-convex, then it is known that (1) has at least one solution [8, Sect. 5.4]. In this case, we denote by $P_C : \mathcal{H} \to C$ a mapping that, given a vector $\mathbf{x}$, always returns a unique point from the solution set of (1).

In the literature, projection methods such as those used later in this work are typically developed for real Hilbert spaces. As it is shown in the following, this is not a restriction when dealing with complex valued signals because the problems we address in complex Hilbert spaces have an equivalent reformulation in a real Hilbert space. The remainder of this section will therefore provide real Hilbert space formulations of concepts that arise in the context of PAPR reduction for complex valued signals.

To this end, consider a complex vector $\underline{\mathbf{v}} \in \mathbb{C}^N$, and define its real Hilbert space equivalent $\mathbf{v}$ by using the following bijective mapping from $\mathbb{C}^N$ to $\mathbb{R}^{2N}$:

$$\mathbf{v} = \mathcal{R}(\underline{\mathbf{v}}) := \left[\text{Re}\{\underline{\mathbf{v}}^T\}, \text{Im}\{\underline{\mathbf{v}}^T\}\right]^T \in \mathbb{R}^{2N}, \tag{2}$$

which concatenates the real- and imaginary part of $\underline{\mathbf{v}}$. In order to represent the multiplication of a matrix $\underline{\mathbf{A}} \in \mathbb{C}^{M \times N}$ by a vector $\underline{\mathbf{v}} \in \mathbb{C}^N$ in a real Hilbert space such that $\mathcal{R}(\underline{\mathbf{A}}\underline{\mathbf{v}}) = \mathcal{R}'(\underline{\mathbf{A}})\mathcal{R}(\underline{\mathbf{v}})$, we define a similar mapping for matrices:

$$\mathbf{A} = \mathcal{R}'(\underline{\mathbf{A}}) := \begin{bmatrix} \mathrm{Re}\{\underline{\mathbf{A}}\} & -\mathrm{Im}\{\underline{\mathbf{A}}\} \\ \mathrm{Im}\{\underline{\mathbf{A}}\} & \mathrm{Re}\{\underline{\mathbf{A}}\} \end{bmatrix} \in \mathbb{R}^{2M \times 2N}. \quad (3)$$

In analogy to the set $\mathcal{I} \subseteq \{1, \ldots, N\}$ indexing elements of a complex vector $\underline{\mathbf{v}}$, we define the index set

$$\mathcal{I}^{\mathbb{R}} = \mathcal{I} \cup \{k \in \mathbb{N} | \; k - N \in \mathcal{I}\}. \quad (4)$$

for indexing real vectors $\mathbf{v} = \mathcal{R}(\underline{\mathbf{v}})$. Note that the standard ℓ_2-norm of a complex vector $\underline{\mathbf{v}}$ is equal to that of its real Hilbert space equivalent $\mathbf{v}$ because

$$\|\underline{\mathbf{v}}\|_2^2 := \sqrt{\underline{\mathbf{v}}^H \underline{\mathbf{v}}} = \|\mathrm{Re}\{\underline{\mathbf{v}}\}\|^2 + \|\mathrm{Im}\{\underline{\mathbf{v}}\}\|^2 = \|\mathbf{v}\|^2. \quad (5)$$

In a complex Hilbert space with elements $\underline{\mathbf{v}} = [\underline{v}_1, \ldots, \underline{v}_N]^T \in \mathbb{C}^N$, the ℓ_∞-norm is given by

$$\|\underline{\mathbf{v}}\|_\infty = \max_{k \in \{1, \ldots, N\}} \sqrt{(\mathrm{Re}\{\underline{v}_k\})^2 + (\mathrm{Im}\{\underline{v}_k\})^2}, \quad (6)$$

and an equivalent notion for the corresponding real Hilbert space can be obtained by defining

$$\|\mathbf{v}\|_{\mathcal{R}_\infty} := \max_{k \in \{1, \ldots, N\}} \sqrt{v_k^2 + v_{k+N}^2} = \|\underline{\mathbf{v}}\|_\infty, \quad (7)$$

which satisfies all properties of a norm in $\mathbb{R}^{2N}$. Given a complex vector $\underline{\mathbf{v}} \in \mathbb{C}^N$ or a complex matrix $\underline{\mathbf{A}} \in \mathbb{C}^{M \times N}$, we use the convention that $\mathbf{v} = \mathcal{R}(\underline{\mathbf{v}})$ and $\mathbf{A} = \mathcal{R}'(\underline{\mathbf{A}})$ throughout the subsequent sections.

B. OFDM System and Basic Definitions

Let $\underline{\mathbf{c}} \in \mathbb{C}^N$ be an OFDM symbol with N subcarriers in the frequency domain, each of them containing a complex valued constellation point. Since peaks in the time-domain signal, which is obtained by applying the inverse discrete Fourier transform to $\underline{\mathbf{c}}$, can increase owing to digital-to-analog conversion, we typically approximate the analog signal by digitally upsampling with a factor of $L \geq 4$ [9]. By doing so, we gain information about the magnitude of peaks in the analog time-domain signal. More precisely, upsampling can be captured by defining a zero-padded vector

$$\hat{\underline{\mathbf{c}}} = \left[\underline{\mathbf{c}}^T, \underline{\mathbf{0}}^T\right]^T \in \mathbb{C}^{NL} \quad (8)$$

and a discrete Fourier transform (DFT) matrix $\underline{\mathbf{F}} \in \mathbb{C}^{NL \times NL}$ with elements

$$\underline{F}_{k,l} = \frac{1}{\sqrt{NL}} e^{-j2\pi \frac{\nu_k t_l}{NL}}, \quad (9)$$

where $(\forall k, l \in \{1, \ldots, NL\})$ $\nu_k = k - N/2 - 1$, and $t_l = l - 1$. The digital approximation of the continuous time-domain signal is thus given by $\underline{\mathbf{F}}^H \hat{\underline{\mathbf{c}}}$. Note that $\underline{\mathbf{F}}$ is normalized such that $\underline{\mathbf{F}}\underline{\mathbf{F}}^H = \underline{\mathbf{F}}^H \underline{\mathbf{F}} = \mathbf{I}$.

A common measure for the distortion on the data subcarriers of a modified version $\underline{\mathbf{x}}$ of a given OFDM symbol $\hat{\underline{\mathbf{c}}}$ is the EVM, defined by

$$\epsilon(\underline{\mathbf{x}}) = \sqrt{\frac{\sum_{k \in \mathcal{I}_{\mathrm{d}}} |\underline{x}_k - \underline{c}_k|^2}{N_{\mathrm{d}} P_0}}, \quad (10)$$

where the set $\mathcal{I}_{\mathrm{d}} = \{i_1, \ldots, i_{N_{\mathrm{d}}}\}$ indicates the N_{d} data subcarriers. In real transceivers, distortions potentially increasing the EVM or the bit error rate (BER) are mainly introduced by peaks exceeding the linear regions of the amplifiers. Therefore, another important signal property of a frequency-domain OFDM symbol $\underline{\mathbf{x}}$ is the PAPR, defined as [5], [10], [11]

$$\mathrm{PAPR}(\underline{\mathbf{x}}) = \frac{\|\underline{\mathbf{F}}^H \underline{\mathbf{x}}\|_\infty^2}{\frac{1}{NL} E(\|\mathbf{S}_{\mathrm{d}}\underline{\mathbf{c}}\|^2)}, \quad (11)$$

where $\mathbf{S}_{\mathrm{d}} = [\mathbf{e}_{i_1}, \ldots, \mathbf{e}_{i_{N_{\mathrm{d}}}}]^T \in \mathbb{R}^{N_{\mathrm{d}} \times N}$ is a row selection matrix for the rows indexed by $\mathcal{I}_{\mathrm{d}}$. If the data subcarriers have an expected power $E(|\underline{c}_i|^2) = P_0$, (11) simplifies to

$$\mathrm{PAPR}(\underline{\mathbf{x}}) = \frac{NL}{N_{\mathrm{d}} P_0} \|\underline{\mathbf{F}}^H \underline{\mathbf{x}}\|_\infty^2. \quad (12)$$

Amplifier non-linearities affect signals with high PAPR more severely, so PAPR reduction methods allow for the deployment of less costly amplifiers. These methods are the topic of the next sections.

III. PAPR REDUCTION BY SET THEORETIC ESTIMATION

In the following section, we formally pose the PAPR problem as a convex feasibility problem in a real Hilbert space $\mathcal{H} = \mathbb{R}^{2NL}$. Subsequently, in Sect. III-B, constraints frequently encountered in the context of PAPR reduction are defined in terms of closed convex sets.

A. Problem Statement

As can be seen in (12), the maximal magnitude of the time-domain signal is directly related to the PAPR. Therefore, given a collection of m convex sets C_i' representing frequency-domain constraints such as the maximal EVM or spectral masks, the PAPR problem can be formulated as the following convex optimization problem in a real Hilbert space $\mathcal{H} = \mathbb{R}^{2NL}$

$$\begin{aligned} \underset{\mathbf{x} \in \mathcal{H}}{\text{minimize}} \quad & \|\mathbf{F}^T \mathbf{x}\|_{\mathcal{R}_\infty} \\ \text{subject to} \quad & \mathbf{x} \in C_{\mathcal{F}} = \bigcap_{i \in S} C_i', \quad S \subseteq \{1, \ldots, m\} \end{aligned} \quad (13)$$

where $\mathbf{F} = \mathcal{R}'(\underline{\mathbf{F}})$ (see (3)). Possible realizations of the sets C_i' will be defined in III-B. A solution $\mathbf{x}^\star$ to the problem in (13) can be obtained with interior point methods, but the complexity may be prohibitive in real-time applications. As a result, simple suboptimal approaches are often used. Examples include ICF [6], TR [4], [5], or the ACE methods [2]. The idea is to reduce the objective value in (13) to a pre-defined threshold value $\theta \geq \|\mathbf{F}^T \mathbf{x}^\star\|_{\mathcal{R}_\infty}$. Formally, these methods replace the problem in (13) by the feasibility problem

$$\underset{\mathbf{x} \in \mathcal{H}}{\text{find}} \; \mathbf{x} \in C_{\mathcal{F}} \cap C_{\mathcal{T}} \quad (14)$$

where $C_{\mathcal{F}} = \bigcap_{i \in S} C_i'$, and $C_{\mathcal{T}} = \{\mathbf{x} \in \mathcal{H} | \; \|\mathbf{F}^T \mathbf{x}\|_{\mathcal{R}_\infty} \leq \theta\}$ is the set of signals bounded by magnitude θ in the time domain. All of the aforementioned techniques can be related to this problem by choosing the constraint set $C_{\mathcal{F}}$ accordingly. If the projection onto $C_{\mathcal{F}}$ is simple to compute, the problem in (14) can be solved with projection methods [8], which only involve operations with low computational complexity, while commonly achieving much of the progress towards the solution during the initial iterations [12].

B. Some Relevant Constraint Sets

This section shows how $C_{\mathcal{F}}$ can be constructed as the intersection of multiple constraint sets C_i', the projections onto which are simple to compute. To this end, we define the following exemplary realizations of the sets C_i' that are commonly used in the literature:

1) Subspace of in-band signals: As the modified OFDM signal is downsampled to the original rate (with subcarriers indexed by the set $\mathcal{I}_{\mathrm{in}} = \{1, \ldots, N\}$) before transmission, the out-of-band radiation (i.e nonzero values in frequency bins exceeding the original bandwidth) caused by clipping needs to be removed. Therefore, the transmit signal should restricted to the subspace

$$C_1' := \{\mathbf{x} \in \mathcal{H} \mid (\forall k \notin \mathcal{I}_{\mathrm{in}}^{\mathbb{R}}), \; x_k = 0\} \quad (15)$$

of in-band signals.

2) Affine subspace of compensation signals: In the TR method, a subset $\mathcal{I}_c \subset \mathcal{I}_{in}$ of the subcarriers is not used for data transmission. These subcarriers transmit dummy symbols that have the sole purpose of decreasing peaks in the time domain [4]. Formally, the corresponding frequency-domain constraint set restricts all but the compensation subcarriers $\mathcal{I}_c$ to their original values:

$$C_2' := \left\{ \mathbf{x} \in \mathcal{H} \mid (\forall k \in \mathcal{I}_{in}^{\mathbb{R}}, k \notin \mathcal{I}_c^{\mathbb{R}}),\ x_k = \hat{c}_k \right\}. \quad (16)$$

3) EVM constraint set: Besides exclusively reserving bandwidth, a degree of freedom for peak cancellation can also be obtained by distorting the data subcarriers. For simplicity, we define $\mathcal{I}_d = \mathcal{I}_{in} \setminus \mathcal{I}_c$. The set of signals with distortion on the data subcarriers bounded by the maximal EVM ϵ_{max} is given by [13]

$$C_3' := \left\{ \mathbf{x} \in \mathcal{H} \mid \sum_{k \in \mathcal{I}_d^{\mathbb{R}}} |x_k - \hat{c}_k|^2 \le (N_d P_0 \epsilon_{max})^2 \right\}. \quad (17)$$

4) ACE constraint set: The idea of active constellation extension is to compensate peaks by allowing boundary points of a square QAM constellation to be moved farther outside, thereby increasing the margin to any other constellation point. While this increases the EVM, the BER can be reduced by this technique [2]. The set of allowable modifications is denoted by

$$C_4' := \bigcap_{k \in \mathcal{I}_d^{\mathbb{R}}} C_{ACE}^k, \quad (18)$$

where, for $\mathbf{x} \in \mathcal{H}$,

$$C_{ACE}^k = \begin{cases} \{\mathbf{x} \mid x_k = \hat{c}_k\}, & \text{if } |\hat{c}_k| \neq \gamma, \\ \{\mathbf{x} \mid \text{sgn}(x_k - \hat{c}_k) = \text{sgn}(\hat{c}_k)\}, & \text{otherwise.} \end{cases} \quad (19)$$

Here, γ is a constant equal to the largest positive real part of all points of the respective QAM constellation.

5) Combining the constraint sets: As mentioned in Sect. III-A, the solution to (14) can be found with projection methods if simple expressions for the projections onto $C_{\mathcal{F}}$ and $C_{\mathcal{T}}$ exist. Some potential combinations of sets C_i' in (14) that have been used in previous studies include the following:

- $S = \{1\}$ (iterative clipping and filtering) [6]
- $S = \{1, 2\}$ (tone reservation) [4]
- $S = \{1, 3, 4\}$ (ACE + EVM + TR) [13]

Further examples for constraint sets are given in [5].

For all combinations mentioned above, a closed form expression for the projection onto $C_{\mathcal{F}}$ exists. In more detail, the projection onto C_4' in (18) can be obtained by composing the projections onto the sets in (19) in arbitrary order (e.g. $P_{C_4'}(\mathbf{x}) = P_{C_{ACE}^{k_{|\mathcal{I}_d^{\mathbb{R}}|}}} \cdots P_{C_{ACE}^{k_1}}(\mathbf{x})$ for $k \in \mathcal{I}_d^{\mathbb{R}}$).

We can show that the projection onto the intersection $C_4' \cap C_3'$ of the sets in (17) and (18) is given by

$$P_{C_4' \cap C_3'}(\mathbf{x}) = P_{C_3'} P_{C_4'}(\mathbf{x}), \quad (20)$$

where order of the projections cannot be changed. We omit the proof due to the page limitation. The projection of a frequency-domain vector $\mathbf{x} \in \mathcal{H}$ onto the set of signals bounded by θ in the time domain is given by

$$P_{C_{\mathcal{T}}}(\mathbf{x}) = \mathbf{F} P_{C_{\theta}}\left(\mathbf{F}^T \mathbf{x}\right), \quad (21)$$

where $P_{C_{\theta}}\left(\mathbf{F}^T \mathbf{x}\right)$ is the projection of a time-domain signal $\mathbf{F}^T \mathbf{x}$ onto the set of signals bounded in time, since projections are defined using the ℓ_2-norm (1), which is invariant under the unitary transformation $\mathbf{F}$. In the following, $P_{\mathcal{F}}(\mathbf{x})$ and $P_{\mathcal{T}}(\mathbf{x})$ denote the projections of $\mathbf{x}$ onto $C_{\mathcal{F}}$ and $C_{\mathcal{T}}$, respectively.

IV. ALGORITHMIC SOLUTIONS

A. Previous Methods

A common method for finding a point within the intersection of closed convex sets is the projections onto convex sets (POCS) algorithm [8]. More precisely, to solve (14), the POCS algorithm produces a sequence $(\mathbf{x}_n)_{n \in \mathbb{N}}$ by

$$\mathbf{x}_{n+1} = P_{\mathcal{F}} P_{\mathcal{T}}(\mathbf{x}_n), \quad \mathbf{x}_0 \in \mathcal{H}, \quad (22)$$

which converges to a point $\mathbf{x}^* \in C_{\mathcal{F}} \cap C_{\mathcal{T}}$ if $C_{\mathcal{F}} \cap C_{\mathcal{T}} \neq \emptyset$. In the PAPR problem, the POCS algorithm iteratively clips $\mathbf{x}_n$ and, subsequently, enforces the frequency-domain constraints specified by $C_{\mathcal{F}}$. Depending on the choice of $C_{\mathcal{F}}$ (see III-B), (22) yields the ICF algorithm [6], the Fourier projection algorithm (FPA) [14], or the ACE-POCS algorithm [2].

In the simplified clipping and filtering (SCF) method [15], the clipping noise $P_{\mathcal{T}}(\mathbf{x}) - \mathbf{x}$ is multiplied by a constant λ in order to achieve strong PAPR reduction within one iteration. For $\lambda \in (0, 2)$ and $C_{\mathcal{F}} = C_{in}$, SCF corresponds to the first iteration of a relaxed POCS algorithm [8]

$$\mathbf{x}_{n+1} = P_{\mathcal{F}}\left(\mathbf{x}_n + \lambda\left(P_{\mathcal{T}}(\mathbf{x}_n) - \mathbf{x}_n\right)\right), \quad (23)$$

which we refer to as rPOCS in the remainder of this study.

B. Extrapolated Method for TR

In the TR scenario, the constraint set $C_{\mathcal{F}}$ is an affine subspace. We exploit this fact by using the EAPM [16] to solve (14). It has been shown in [12], that the EAPM converges considerably faster than the POCS algorithms in (22) and (23) for affine-convex feasibility problems. Given a point $\mathbf{x}_0 \in C_{\mathcal{F}}$ in an affine subspace $C_{\mathcal{F}} \subset \mathcal{H}$ of a real Hilbert space, and a closed convex set $C_{\mathcal{T}} \subset \mathcal{H}$, the EAPM algorithm generates a sequence $(\mathbf{x}_n)_{n \in \mathbb{N}}$ by

$$\mathbf{x}_{n+1} = \mathbf{x}_n + \lambda_n K_n \left(P_{\mathcal{F}} P_{\mathcal{T}}(\mathbf{x}_n) - \mathbf{x}_n\right), \quad (24)$$

with $\lambda_n \in (0, 2)$ and an extrapolation factor

$$K_n = \frac{\|P_{\mathcal{T}}(\mathbf{x}_n) - \mathbf{x}_n\|^2}{\|P_{\mathcal{F}} P_{\mathcal{T}}(\mathbf{x}_n) - \mathbf{x}_n\|^2}. \quad (25)$$

If $C_{\mathcal{F}} \cap C_{\mathcal{T}} \neq \emptyset$, convergence to a point $\mathbf{x}^* \in C_{\mathcal{F}} \cap C_{\mathcal{T}}$ is guaranteed. As we show in the Appendix, the EAPM is a particular case of the adaptive projected subgradient method (APSM) [17], which has also been used in [5] for PAPR reduction with TR constraints.

C. PAPR Reduction with Arbitrary Constraints

Imposing EVM or ACE constraints results in a non-affine set $C_{\mathcal{F}}$. In this case, the EAPM algorithm cannot be used because extrapolation might cause the iterate $\mathbf{x}_n$ to violate the frequency-domain constraints. To circumvent this issue, we propose a PAPR reduction technique for non-affine frequency-domain constraints based on the GPR approach [7]. Given two arbitrary closed convex sets $C_{\mathcal{F}}, C_{\mathcal{T}} \subset \mathcal{H}$ in a finite dimensional Hilbert space, the GPR algorithm produces a sequence $(\mathbf{x}_n)_{n \in \mathbb{N}}$ by

$$\mathbf{x}_{n+1} = P_{\mathcal{F}}\left(\mathbf{x}_n + \lambda_n \sigma_n^{GPR}\left(P_{\mathcal{F}} P_{\mathcal{T}}(\mathbf{x}_n) - \mathbf{x}_n\right)\right), \quad (26)$$

where

$$\sigma_n^{GPR} = \frac{\|P_{\mathcal{T}}(\mathbf{x}_n) - \mathbf{x}_n\|^2}{\langle P_{\mathcal{F}} P_{\mathcal{T}}(\mathbf{x}_n) - \mathbf{x}_n, P_{\mathcal{T}}(\mathbf{x}_n) - \mathbf{x}_n \rangle} \quad (27)$$

is an extrapolation factor established in [18]. As in the case of the EAPM, convergence to a point $\mathbf{x}^* \in C_{\mathcal{F}} \cap C_{\mathcal{T}}$ is guaranteed if the intersection is non-empty.

If $C_{\mathcal{F}}$ is affine, σ_n^{GPR} in (27) equals K_n in (25), since $\langle P_{\mathcal{F}} P_{\mathcal{T}}(\mathbf{x}) - \mathbf{x}, P_{\mathcal{T}}(\mathbf{x}) - P_{\mathcal{F}} P_{\mathcal{T}}(\mathbf{x}) \rangle = 0$ for affine subspaces $C_{\mathcal{F}}$. In this case, the algorithm in (26) is identical to the EAPM in (24). Therefore, it can be seen as a generalization of the EAPM for arbitrary closed convex sets $C_{\mathcal{F}}$.

Consequently, the GPR algorithm can be used for PAPR reduction with arbitrary combinations of the constraint sets defined in Sect. III-B. The constraints can be altered on-line, without the necessity to change the structure of the algorithm. If the set $C_{\mathcal{F}}$ is affine, the performance is equivalent to that of the EAPM, whereas for non-affine constraints, the method is still applicable and yields rapid PAPR reduction. A further property of this approach is that, due to the final unrelaxed projection onto $C_{\mathcal{F}}$, the iterate $\mathbf{x}_n$ satisfies the frequency-domain constraints at each iteration.

Note also that the computational complexity of one iteration is roughly equal for all algorithms considered in Sect. IV, since each iteration involves one projection onto $C_{\mathcal{T}}$, and therefore one IDFT/DFT-pair.

D. Phaseless Pilot Reuse

A recent branch of research in OFDM channel estimation is directed towards the deployment of phaseless pilots [19], [20], which allow the receiver to reconstruct the phase shift introduced by the wireless channel without requiring knowledge of the pilot phases. This channel estimation scheme enables the transmitter to use the phase of the pilot subcarriers for peak compensation.

In this scheme, the set of pilot subcarriers is identical with the set $\mathcal{I}_{\mathrm{c}}$ of compensation subcarriers. While in the various definitions of $C_{\mathcal{F}}$ in Sect. III-B there was no constraint on the compensation subcarriers, simultaneously using them as phaseless pilots imposes an equality constraint on their magnitude. This is taken into account by defining the non-convex set

$$C_P := \left\{ \mathbf{x} \in \mathbb{R}^{2NL} \mid (\forall k \in \mathcal{I}_{\mathrm{c}}),\ x_k^2 + x_{k+NL}^2 = p_k \right\}, \quad (28)$$

where p_k denotes the power of the kth subcarrier. The problem in (14) is then extended to the non-convex feasibility problem

$$\underset{\mathbf{x} \in \mathcal{H}}{\text{find}}\ \mathbf{x} \in C_{\mathcal{F}} \cap C_{\mathcal{T}} \cap C_P, \quad (29)$$

which is solved heuristically by terminating each iteration of the above algorithms by a projection onto C_P. Formally, if $\mathbf{x}_{n+1} = T(\mathbf{x}_n)$ denotes the update rule of any of the algorithms in (22), (23), (24) or (26), the equality constraint on the magnitude of the subcarriers in $\mathcal{I}_{\mathrm{c}}$ can be incorporated by

$$\mathbf{x}_{n+1} = P_{C_P} T(\mathbf{x}_n). \quad (30)$$

Note that, although it is a non-convex set, the projection of $\mathbf{x}$ onto C_P is unique if $\forall k \in \mathcal{I}_{\mathrm{c}}: x_k^2 + x_{k+NL}^2 \neq 0$.

A very similar non-convex heuristic has been proposed in [21] for PAPR reduction in pulse amplitude modulated transform domain communication systems.

E. Practical Aspects: Feasibility, Computational Efficiency

As mentioned above, convergence of the extrapolated methods in (24) and (26) is only guaranteed if θ is chosen such that $C_{\mathcal{F}} \cap C_{\mathcal{T}} \neq \emptyset$. One way of achieving this is to use bisection search as proposed in [12]. This might however lead to a slower decrease in PAPR because an appropriate value for θ has to be found first.

In practice, only a small number of iterations can be computed before transmitting the symbol. It is therefore desirable to have a good choice for θ from the first iteration. This can be achieved by running several instances of the algorithm with different clipping thresholds θ in parallel, and outputting the result with lowest PAPR after the last iteration. In case the computational resources are very restricted, it is also possible to use only one instance of the algorithm in (26) with a clipping threshold chosen such that the probability of the problem in (14) being infeasible is sufficiently small. To avoid
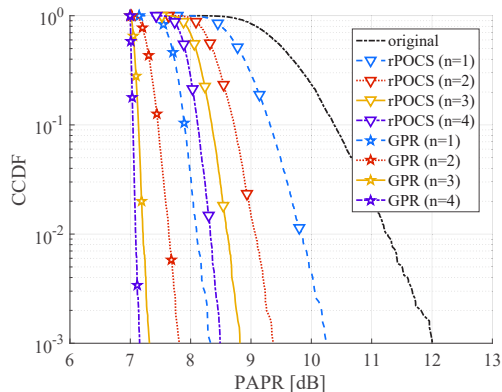

Fig. 1. Complementary PAPR CDF for the first four iterations of relaxed POCS ($\lambda_{\mathrm{POCS}} = 2$) and GPR ($\lambda_{\mathrm{GPR}} = 1.4$) with ACE constraints, $N = 2048$, $L = 4$, CR $= 7\,\mathrm{dB}$, $5\,\%$ compensation subcarriers, data subcarriers modulated with QPSK and 16-QAM, respectively, where $\mathrm{EVM}_{\mathrm{QPSK}}^{\max} = 15\,\%$ and $\mathrm{EVM}_{\mathrm{QAM}}^{\max} = 5\,\%$.

the extrapolating algorithm to increase the PAPR in these few remaining cases, we can compare the extrapolated result to that without extrapolation, and output the one with lower PAPR.

While the projection methods mentioned above produce sequences $(\mathbf{x}_n)_{n \in \mathbb{N}}$ that converge to a feasible point $\mathbf{x}^*$, as $n \to \infty$, the computational resources of the transmitter often only allow for computing a single iteration. This fact is taken into account by the SCF algorithm [15], which computes a single overrelaxed POCS iteration instead of multiple unrelaxed POCS iterations (ICF). The SCF approach relies on a fixed overrelaxation/extrapolation parameter λ that may be larger than two, in which case the algorithm loses its convergence guarantee. A further disadvantage of SCF is that it lacks a means of controlling the in-band distortion introduced by the peak compensation. The BER of the system will therefore greatly depend on the choice of clipping threshold θ and relaxation/extrapolation parameter λ. In contrast, the algorithm in (26) produces a sequence of symbols each of them satisfying all constraints in the frequency domain. For example, individual EVM constraints can be specified for subcarriers conveying constellations of different size. In this way, the distortion is restricted independently of the choice of clipping threshold and relaxation parameter. Furthermore, the extrapolation factor σ_n^{GPR} is chosen adaptively, so computing one iteration according to (26) can reduce the PAPR by an amount similar to that achieved by the SCF method, while not losing the convergence guarantee if multiple iterations can be computed to refine the estimate.

V. SIMULATIONS

In this section, we compare the performance of the algorithms in (23) and (26), in the following denoted as rPOCS and GPR, respectively. The simulation is performed for randomly generated OFDM symbols with $N = 2048$ subcarriers. Negative frequency subcarriers convey QPSK constellation points, whereas positive frequency subcarriers convey 16-QAM constellation points. For each symbol, $5\,\%$ of the subcarriers are randomly selected as compensation subcarriers. Data subcarriers are required to satisfy both EVM and ACE constraints, where $\mathrm{EVM}_{\mathrm{QPSK}}^{\max} = 15\,\%$ and $\mathrm{EVM}_{\mathrm{QAM}}^{\max} = 5\,\%$, respectively. Peaks in the analog signal were approximated by upsampling by a factor $L = 4$, and clipped at a clipping ratio (target PAPR) of CR $= 7\,\mathrm{dB}$. The relaxation parameter
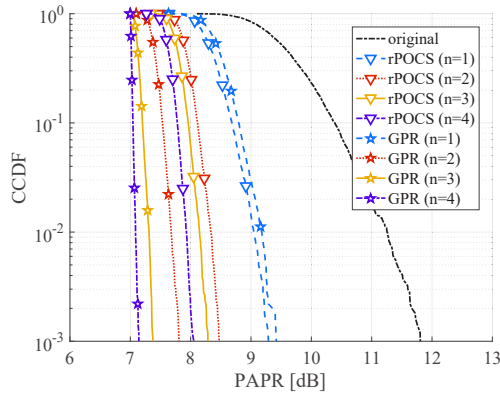
Fig. 2. CCDF for the same simulation setup as in Fig. 1, where each iteration is terminated by an additional projection onto the non-convex set C_P according to (30), with $p_k = 1 \; \forall k \in \mathcal{I}_c$.

for the GPR algorithm was set to $\lambda_{\mathrm{GPR}} = 1.4$, although rapid decrease in PAPR was observed for any $\lambda_{\mathrm{GPR}} \in [1, 2]$. As large overrelaxation yielded the fastest PAPR decrease for the rPOCS method, the relaxation parameter was set to $\lambda_{\mathrm{POCS}} = 2$. Note that, by definition, all of the frequency-domain constraints are satisfied in every iteration.

Fig. 1 shows the complementary cumulative distribution function (CCDF) of the PAPR for the first four iterations of both algorithms. It can be seen that, for rPOCS, the rate of convergence decreases at every iteration. The GPR algorithm achieves almost $2 \, \mathrm{dB}$ lower PAPR than rPOCS in the first iteration, while almost reaching the target PAPR after four iterations. Fig. 2 shows the CCDF for the same scenario, for the pilot reuse scheme described in Sect. IV-D. It can be seen that adding the additional magnitude constraint on pilot/compensation subcarriers does not decrease the speed of convergence.

VI. CONCLUSION

In this work, we proposed a PAPR reduction algorithm for TR based on the EAPM, as well as its generalization for non-affine frequency-domain constraints, which is based on the GPR approach. In addition, we proposed a heuristic extension for non-convex constraints that allows reusing the phase of pilot subcarriers for phaseless channel estimation to reduce the PAPR. Simulations showed that the proposed methods were able to decrease greatly the PAPR with very few iterations.

APPENDIX

In the following, we show that the EAPM [16] is a particular case of the embedded constraint version of the APSM [17, Example 5], which produces a sequence $(\mathbf{x}_n)_{n \in \mathbb{N}}$ by

$$\mathbf{x}_{n+1} = \mathbf{x}_n - \lambda_n \frac{\Theta_n(\mathbf{x}_n)}{\|P_M(\Theta'(\mathbf{x}_n))\|^2} P_M(\Theta'(\mathbf{x}_n)), \qquad (31)$$

where $M \subset \mathcal{H} = \mathbb{R}^{2NL}$ is a linear subspace such that $C_{\mathcal{F}} = M + \mathbf{v}$. While the cost function Θ_n can be changed in each iteration, we choose a fixed cost function $(\forall n \in \mathbb{N}) \; \Theta_n(\mathbf{x}) = \|\mathbf{x} - P_{C_{\mathcal{T}}}(\mathbf{x})\|$, a subgradient of which is given by

$$\Theta'_n(\mathbf{x}) = \frac{\mathbf{x} - P_{C_{\mathcal{T}}}(\mathbf{x})}{\|\mathbf{x} - P_{C_{\mathcal{T}}}(\mathbf{x})\|} \in \partial \Theta_n(\mathbf{x}),$$

where $C_{\mathcal{T}} \subset \mathcal{H}$ is a closed convex set. Because $C_{\mathcal{F}}$ is an affine subspace, it holds that [8, p. 155]

$$\left(\exists \mathbf{A} \in \mathbb{R}^{2NL \times 2NL} \right), \left(\exists \mathbf{b} \in \mathcal{H} \right) : P_{C_{\mathcal{F}}}(\mathbf{x}) = \mathbf{A}\mathbf{x} + \mathbf{b},$$

where $\mathbf{b} = P_{C_{\mathcal{F}}}(\mathbf{0}) = \mathbf{v}$. Thus

$$P_M\left(\Theta'_n(\mathbf{x}_n)\right) = P_{C_{\mathcal{F}}}(\Theta'_n(\mathbf{x}_n)) - \mathbf{b}$$

$$= \mathbf{A}\frac{(\mathbf{x}_n - P_{C_{\mathcal{T}}}(\mathbf{x}_n))}{\|\mathbf{x}_n - P_{C_{\mathcal{T}}}(\mathbf{x}_n)\|} = \frac{\mathbf{A}\mathbf{x}_n + \mathbf{b} - (\mathbf{A}P_{C_{\mathcal{T}}}(\mathbf{x}_n) + \mathbf{b})}{\|\mathbf{x}_n - P_{C_{\mathcal{T}}}(\mathbf{x}_n)\|}$$

$$= \frac{P_{C_{\mathcal{F}}}(\mathbf{x}_n) - P_{C_{\mathcal{F}}}P_{C_{\mathcal{T}}}(\mathbf{x}_n)}{\|\mathbf{x}_n - P_{C_{\mathcal{T}}}(\mathbf{x}_n)\|} = \frac{\mathbf{x}_n - P_{C_{\mathcal{F}}}P_{C_{\mathcal{T}}}(\mathbf{x}_n)}{\|\mathbf{x}_n - P_{C_{\mathcal{T}}}(\mathbf{x}_n)\|},$$

where the last equality follows from the fact that $(\forall n \in \mathbb{N})$ $\mathbf{x}_n \in C_{\mathcal{F}}$. Substituting in (31) yields

$$\mathbf{x}_{n+1} = \mathbf{x}_n + \lambda_n \frac{\|\mathbf{x}_n - P_{C_{\mathcal{T}}}(\mathbf{x}_n)\|^2}{\|\mathbf{x}_n - P_{C_{\mathcal{F}}}P_{C_{\mathcal{T}}}(\mathbf{x}_n)\|^2} \left(P_{C_{\mathcal{F}}}P_{C_{\mathcal{T}}}(\mathbf{x}_n) - \mathbf{x}_n \right),$$

which is the definition of the EAPM algorithm in (24).

REFERENCES

[1] G. Wunder, R. F. Fischer, H. Boche, S. Litsyn, and J.-S. No, "The papr problem in OFDM transmission: New directions for a long-lasting problem," *IEEE Signal Processing Magazine*, vol. 30, no. 6, pp. 130–144, 2013.

[2] B. S. Krongold and D. L. Jones, "PAR reduction in OFDM via active constellation extension," *IEEE Transactions on broadcasting*, vol. 49, no. 3, pp. 258–268, 2003.

[3] Y. Rahmatallah and S. Mohan, "Peak-to-average power ratio reduction in OFDM systems: A survey and taxonomy," *IEEE communications surveys & tutorials*, vol. 15, no. 4, pp. 1567–1592, 2013.

[4] J. Tellado and J. M. Cioffi, "Peak power reduction for multicarrier transmission," in *IEEE GLOBECOM*, vol. 99, 1998, pp. 5–9.

[5] R. L. Cavalcante and I. Yamada, "A flexible peak-to-average power ratio reduction scheme for OFDM systems by the adaptive projected subgradient method," *IEEE Transactions on Signal Processing*, vol. 57, no. 4, pp. 1456–1468, 2009.

[6] J. Armstrong, "Peak-to-average power reduction for OFDM by repeated clipping and frequency domain filtering," *Electronics letters*, vol. 38, no. 5, pp. 246–247, 2002.

[7] A. Cegielski, *Iterative methods for fixed point problems in Hilbert spaces*. Springer, 2012, vol. 2057.

[8] H. Stark, Y. Yang, and Y. Yang, *Vector space projections: a numerical approach to signal and image processing, neural nets, and optics*. John Wiley & Sons, Inc., 1998.

[9] M. Sharif, M. Gharavi-Alkhansari, and B. H. Khalaj, "On the peak-to-average power of OFDM signals based on oversampling," *IEEE Transactions on Communications*, vol. 51, no. 1, pp. 72–78, 2003.

[10] B. S. Krongold and D. L. Jones, "An active-set approach for OFDM PAR reduction via tone reservation," *IEEE transactions on signal processing*, vol. 52, no. 2, pp. 495–509, 2004.

[11] A. T. Erdogan, "A low complexity multicarrier PAR reduction approach based on subgradient optimization," *Signal Processing*, vol. 86, no. 12, pp. 3890–3903, 2006.

[12] Y. Censor, W. Chen, P. L. Combettes, R. Davidi, and G. T. Herman, "On the effectiveness of projection methods for convex feasibility problems with linear inequality constraints," *Computational Optimization and Applications*, vol. 51, no. 3, pp. 1065–1088, 2012.

[13] A. Aggarwal and T. H. Meng, "Minimizing the peak-to-average power ratio of OFDM signals via convex optimization," in *Global Telecommunications Conference, 2003. GLOBECOM'03. IEEE*, vol. 4. IEEE, 2003, pp. 2385–2389.

[14] A. Gatherer and M. Polley, "Controlling clipping probability in DMT transmission," in *Signals, Systems & Computers, 1997. Conference Record of the Thirty-First Asilomar Conference on*, vol. 1. IEEE, 1997, pp. 578–584.

[15] L. Wang and C. Tellambura, "A simplified clipping and filtering technique for PAR reduction in OFDM systems," *IEEE signal processing letters*, vol. 12, no. 6, pp. 453–456, 2005.

[16] H. H. Bauschke, P. L. Combettes, and S. G. Kruk, "Extrapolation algorithm for affine-convex feasibility problems," *Numerical Algorithms*, vol. 41, no. 3, pp. 239–274, 2006.

[17] I. Yamada and N. Ogura, "Adaptive projected subgradient method for asymptotic minimization of sequence of nonnegative convex functions," *Numerical Functional Analysis and Optimization*, vol. 25, no. 7-8, pp. 593–617, 2005.

[18] L. Gurin, B. Polyak, and E. Raik, "The method of projections for finding the common point of convex sets," *USSR Computational Mathematics and Mathematical Physics*, vol. 7, no. 6, pp. 1–24, 1967.

[19] P. Walk, H. Becker, and P. Jung, "OFDM channel estimation via phase retrieval," in *Signals, Systems and Computers, 2015 49th Asilomar Conference on*. IEEE, 2015, pp. 1161–1168.

[20] ——, "Phaseless pilots for OFDM," in *Wireless Communication Systems (ISWCS), 2015 International Symposium on*. IEEE, 2015, pp. 86–90.

[21] R. K. Martin and M. Haker, "Reduction of peak-to-average power ratio in transform domain communication systems," *IEEE Transactions on Wireless Communications*, vol. 8, no. 9, 2009.